JSRP1 **variants affect skeletal muscle excitation contraction coupling by decreasing the**

sensitivity of the dihydropyridine receptor

Toshimichi Yasuda[1], Osvaldo Delbono[2], Zhong-Min Wang[2], Maria L. Messi[2], Thierry Girard[3], Albert Urwyler[3], Susan Treves,[3,4*] and Francesco Zorzato[3,4]

1. Department of Anesthesiology and Critical Care, Hiroshima University, 1-2-3 Kasumi, Manami-ku, Hiroshima 734-8511, Japan.

2. Department of Internal Medicine, Gerontology and Geriatric Medicine, Wake Forest School of Medicine, Medical Center Boulevard, Winston-Salem, NC 27157, U.S.A.

3. Departments of Anesthesia and Biomedizin, Basel University Hospital, Hebelstrasse 20, 4031 Basel, Switzerland.

4. Department of Experimental and Diagnostic medicine, General Pathology section, Via Borsari 46, 44100 Ferrara, Italy.

*Corresponding Author:

Susan Treves

Basel University Hospital

Anesthesia and Research

Hebelstrasse 20

Basel

4031

Switzerland

Phone: +41-61-265-2373

Fax: +41-61-265-3702

E-mail: susan.treves@unibas.ch

ABSTRACT

JP-45 is an integral protein constituent of the skeletal muscle sarcoplasmic reticulum junctional face membrane interacting with $Ca_v1.1$ (the $\alpha.1$ subunit of the voltage sensing dihydropyridine receptor) and the luminal calcium-binding protein calsequestrin. Two *JSRP1* variants have been found in the human population: c.323C>T (p.P108L) in exon 5 and c.449G>C (p.G150A) in exon 6, but nothing is known concerning the incidence of these polymorphisms in the general population or in patients with neuromuscular diseases nor the impact of the polymorphisms on excitation-contraction coupling. In the present report we investigated the frequencies of these two *JSRP1* polymorphisms in the Swiss Malignant Hyperthermia population and studied the functional impact of the variants on excitation -contraction coupling. Our results show that the polymorphisms are equally distributed among Malignant Hyperthermia Negative, Malignant Hyperthermia Equivocal and Malignant Hyperthermia Susceptible individuals. Interestingly however, the presence of either one of these JP-45 variants decreased the sensitivity of the dihydropyridine receptor to activation. The presence of a *JSRP1* variant may explain the variable phenotype seen in patients with malignant hyperthermia carrying the same mutation and more importantly, may counteract the hypersensitivity of excitation-contraction coupling caused by mutations in the *RYR1* gene.

Key Words: JP-45, dihydropyridine receptor, excitation-contraction coupling, polymorphisms, down regulation, skeletal muscle.

INTRODUCTION

Skeletal muscle excitation-contraction (EC) coupling is a physiological process whereby an electrical signal (depolarization of the plasma membrane) is converted into a chemical signal, i.e. a calcium gradient, by the opening of ryanodine receptor (RyR1) Ca^{2+} release channels located on the sarcoplasmic reticulum (SR) terminal cisternae. The Ca^{2+} then binds to the contractile proteins to initiate muscle contraction; muscle relaxation occurs when the myoplasmic Ca^{2+} is pumped back into the SR by the activity of the SERCA CaATPases (Fleischer and Inui, 1989; Rios and Pizarro, 1991; Franzini-Armstrong and Jorgensen, 1994). The two core components of the EC coupling machinery are the voltage sensing dihydropyridine receptor (DHPR) Ca^{2+} channel located on the transverse tubules and the RyR1. Upon sensing a change in voltage the DHPR undergoes a conformational change whereby it directly interacts with and activates the RyR1, causing Ca^{2+} release from the SR ((Nakai et al., 1996; Sutko and Airey, 1996). The activity of the DHPR can be measured electrophysiologically and is accompanied by a measurable intermembrane current, which is proportional to the movement of charged ions across the transverse tubular membrane (Schneider and Chandler, 1973; Adams et al., 1990).

Several congenital neuromuscular disorders are linked to dysregulation of calcium homeostasis among which the subclinical myopathy Malignant Hyperthermia (MH; MIM# 145600), the congenital core myopathy Central core disease (CCD; MIM# 117000) and some forms of Multiminicore disease (MmD; MIM# 255320) Centronuclear myopathy (CNM; MIM# 160150) and Congenital fiber type disproportion (Treves et al., 2008, Jungbluth et al., 2011; Wilmhurst et al., 2011; Clarke et al., 2010). Though more than 200 mutations in the *RYR1* gene have been identified in patients belonging to these disease categories (Robinson et al., 2006;

Jungbluth et al., 2011; Duarte et al., 2011), analysis of other genes encoding proteins involved in EC coupling have so far identified only mutations in *CACNA1S,* the gene encoding the $\alpha 1$ subunit ($Ca_v1.1$) of the skeletal muscle dihydropyridine receptor (DHPR) to be causatively linked to the pharmacogenetic disorder MH (Monnier et al., 1997; Stewart et al., 2001; Pirone et al., 2010; Toppin et al., 2010). However mutations in these genes only accounts for approximately 70-80 % of the human cases and the search for mutations in other genes encoding proteins involved in EC coupling has so far yielded few if any true positive candidates.

Malignant Hyperthermia is a subtle pharmacogenetic disorder triggered by halogenated anesthetics and the muscle relaxant succinylcholine in genetically predisposed individuals (Glahn et al., 2010; Robinson et al., 2006; Treves et al., 2008). In their everyday life such individuals are unaware of their condition though a small number of them may suffer from heat intolerance, muscle cramping after intense exercise and rhabdomyolysis; however, once such individuals come in contact with a trigger agent they undergo a rapid hypermetabolic reaction which is often fatal if left untreated. Thus, identifying potentially susceptible patients and their relatives prior to contact with a anesthesia is of utmost importance and the aim of clinical MH-related research for non-invasive testing. In the past few years novel proteins of the SR have been identified and in many cases their ablation has been shown to affect Ca^{2+} homeostasis and/or muscle performance. In previous studies we identified JP-45, an integral membrane protein of skeletal muscle SR junctional face membrane which interacts via its amino terminal with $Ca_v1.1$ and via its carboxy terminal, with the luminal calcium binding protein calsequestrin (Anderson et al., 2003, 2006). Three months old JP-45 mice showed decreased muscle strength, a decrease of the functional expression of the $Ca_v1.1$ and a decrease of depolarization-induced Ca^{2+} release (Delbono et al., 2007). These changes however, were no longer evident in old (>12

month old) JP-45 KO mice (Delbono et al., 2012). An initial study aimed at screening the *JSRP1* gene (MIM# 608743), the gene encoding JP-45, showed the existence of two JP-45 variants (dbSNP and Exome Variant Server NHLBI Exome Sequencing Project databases): c.323C>T (exon 5) resulting in the p.P108L substitution (dbSNP database accession NM144616.3 and NP 653217.1; rs74521370) and c.449G>C resulting in the p.G150A substitution (exon 6) (dbSNP data accession NM 144616.3 and NP653217.1; rs 80043033) (Althobiti et al. 2009); because of the prevalence of the latter polymorphism in MH susceptible individuals it was hypothesized that such variants may serve as "function modifiers", but no information as to how this could be accomplished was provided.

In the present study we investigated (i) the frequency of the two JP-45 variants in the Swiss MH population and (ii) the effect of the polymorphisms on EC coupling. Our results show that though the distribution does not vary significantly between MH negative (MHN), MH equivocal (MHE) and MH susceptible (MHS) individuals, the presence of either the p.P108L or the p.G150A variant affects the functional properties of the voltage sensor, without directly affecting the functional properties of the RyR1. Thus the presence of *JSRP1* variants may downregulate the activity of the EC coupling machinery and may account for some of the phenotypic differences seen in individuals carrying the same *RYR1* mutation.

MATERIALS AND METHODS

Patient selection and genomic DNA isolation

Patients referred to the Swiss MH investigation unit (Department of Anesthesia, University Hospital Basel, Switzerland) for MH screening using an open muscle biopsy were included in this study. All patients gave their written informed consent for storing their muscle tissue, establishing primary muscle cell cultures and using DNA obtained from a blood sample for research projects specifically focusing on MH. This procedure was approved by the Ethics Committee of the University Hospital Basel. The patients were classified into MHN (Malignant hyperthermia negative), MHE (MH equivocal) and MHS (MH susceptible) by the vitro contracture test (IVCT) on isolated muscle strips of the open muscle biopsy obtained from the vastus medialis or lateralis muscles under regional anesthesia. The IVCT was performed according to the protocol of the European MH Group (EMHG, 1984). Individuals were diagnosed as MHS if a contracture of 0.2 g or greater occurred at 2 mM caffeine or less and 2% halothane or less. An MHN diagnosis was established if a contracture of 0.2 g was not reached by 2 mM caffeine and 2% halothane. An MH equivocal (MHE) diagnosis was made if a contracture of 0.2 g or greater occurred only at 2 mM caffeine or less (MHEc) or 2% halothane or less (MHEh) but not with both testing substances. Patients were also screened for the presence of *RYR1* mutations included in the EMHG guidelines as previously described (Girard et al. 2001). MH testing was approved by the ethical board of the Basel University Hospital. The presence of the *JSRP1* polymorphic variants was assayed on genomic DNA isolated either from whole blood or untreated muscle tissue using QIAamp DNA mini kit (Qiagen AG) following the manufacturers recommendations.

Identification of *JSRP1* variants

The following primers and conditions were used to amplify JP-45 from genomic DNA: exon F 5'-ACAGAGCCAGTGACCACAGC-3' and R 5' –GAGGAATAGGCGCACAGGT-3'; exon 6 F 5'-GAGGGATGGACAGTGTGGAC-3' and R 5'-CTTTCCTTGGGGATGAAGGT-3'. Amplification conditions were 1 cycle 95°C 4 min followed by 35 cycles annealing (65°C c.323C>T and 63°C for c.449G>C, 45 sec), extension (72°C, 40 sec), denaturation (95°C, 30 sec), followed by a 5 min extension cycle at 72°C. The PCR-amplified DNA fragments were purified using Qiagen PCR purification columns, digested with MspA1l (c.323C>T in exon 5) or AciI (c.449G>C in exon 6) run on a 15% acrylamide gel and visualized by ethidium bromide staining. The DNA mutation numbering system is based on the cDNA reference sequence, with +1 as the A of the initiator ATG codon..

Human myotube cultures and intracellular Ca^{2+} measurements

primary skeletal muscle cultures were established from fragments of muscle biopsies obtained from patients undergoing diagnostic testing, as previously described (Ducreux et al., 2004)**.** Cells were cultured on 0.17 mm thick glass coverslips in growth medium and induced to differentiate into myotubes by culturing them in DMEM plus 4.5 mg/ml glucose, 0.5% BSA, 10 ng/ml EGF, 0.15 mg/ml creatine, 5 ng/ml insulin, 200 mM glutamine, 600 ng/ml penicillin G and streptomycin, and 7 mM HEPES, pH 7.4 for 7-10 days.

For cytoplasmic calcium measurements, coverslip grown myotubes were either loaded with the ratiometric fluorescent Ca^{2+} indicator fura-2-AM or Fluo-4 AM (final concentration 5 µM) in differentiation medium for 30 min at 37°C, after which the coverslips were mounted onto a 37°C thermostatically controlled chamber which was continuously perfused with Krebs-Ringer

medium. On-line measurements were recorded using a fluorescent Axiovert S100 TV inverted microscope (Carl Zeiss GmbH, Jena, Germany) equipped with a 20x water-immersion FLUAR objective (0.17 NA), filters (BP 340/380, FT 425, BP 500/530) and attached to a Cascade 125+ CCD camera or with a Nikon TE2000 TIRF microscope equipped with a dry 20x Plan Fluor objective (0.17 N.A.), filters (ex 472/3; em 488, BP 525/30) and an electron multiplier Hamamatsu CCD C9100-13 camera as previously described (Treves et al., 2010). Changes in fluorescence were analyzed using Metamorph imaging system and the average pixel value for each cell was measured as previously described (Ducreux et al., 2004, Treves et al., 2010). Individual cells were stimulated by means of a 12- or 8-way 100 mm diameter quartz micromanifold computer controlled microperfuser (ALA Scientific instruments, Westbury N.Y. U.S.A.), as previously described (Ducreux et al., 2004).

Electroporation of muscles from JP-45 KO mice with the cDNA carrying the variants in exon 5 or exon 6

JP-45KO mice were used for plasmid electroporation according to DiFranco et al. (2006). Briefly, *flexor digitorum brevis* (FDB) muscles were injected with 5 µl of 2mg/ml hyaluronidase and injected 1 hour later with 20 µg DsRed-conjugated JP-45 mutants or wild-type cDNAs. Ten minutes later, two sterile, gold-plated acupuncture needles were placed under the skin on adjacent sides of the muscle. Twenty 100 V/cm, 20-ms square-wave pulses of 1-Hz frequency were applied to the muscle for one second each using a Grass stimulator (Grass S48; W. Warwick, RI, USA).

Charge movement and calcium current recordings

FDB muscle fibers were transferred to a small flow-through Lucite chamber positioned on a microscope stage. Fibers were continuously perfused with the external solution (see below) using a push-pull syringe pump. Only fibers exhibiting clean surface and lack of evidence of contracture were used for electrophysiological recordings. Muscle fibers were voltage-clamped using an Axopatch-200B amplifier (Molecular Devices) in the whole-cell configuration of the patch-clamp technique (Hamill et al., 1981; Delbono et al., 2007). Patch pipettes were pulled from borosilicate glass (Boralex) using a Flaming Brown micropipette puller (P97, Sutter Instrument Co., Novato, CA) and then fire-polished to obtain electrode resistance ranging from 450 to 650 $k\Omega$. In cell-attached the seal resistance was in the range of 1 to 4.5 $G\Omega$ (n = 50) and in the whole-cell configuration the values were between ~100 $M\Omega$. Only experiments with resistance more than 100 $M\Omega$ were included in the analysis. The pipette was filled with the following solution (mM): 140 Cs-aspartate; 2 Mg-aspartate$_2$, 0.2 or 10 Cs$_2$EGTA (ethylene glycol-bis(α-aminoethyl ether)-N,N,N'N'-tetraacetic acid), 10 HEPES (N-[2-hydroxyethyl]piperazine-N'-[2-ethanesulfonic acid]), pH was adjusted to 7.4 with CsOH (Adams et al., 1990). The external solution used for Ca^{2+} current recording contained (mM): 150 TEA(tetraethylammonium hydroxide)-CH$_3$SO$_3$, 2 MgCl$_2$, 2 CaCl$_2$, 10 Na-HEPES and 0.001 tetrodotoxin (Delbono, 1992). Solution pH was adjusted to 7.4 with CsOH. Both, the pipette and the bath solution, were selected based on the ease of membrane seal formation and cell stability over time. For charge movement recording, Ca^{2+} current was blocked with the external solution containing 0.5 mM Cd^{2+} and 0.3 mM La^{3+} (Adams et al., 1990).

Whole-cell currents were acquired and filtered at 5 kHz with pCLAMP 10 software (Molecular Devices). A Digidata 1440A interface (Molecular Devices) was used for A-D conversion. Membrane current during a voltage pulse, P, was initially corrected by analog

10

subtraction of linear components. The remaining linear components were digitally subtracted on-line using hyperpolarizing control pulses of one-quarter test pulse amplitude (-P/4 procedure) as previously described for mouse muscle fibers (Delbono, 1992). Four control pulses were applied before the test pulse. Charge movements were evoked by 25 ms depolarizing pulses from the holding potential (-80 mV) to command potentials ranging from −70 to 60 mV with 10mV interval. Intramembrane charge movement was calculated as the integral of the current in response to depolarizing pulses (charge on, Q_{on}) and is expressed per membrane capacitance (coulombs per farad). The complete blockade of the inward Ca^{2+} current was verified by the Q_{on} − Q_{off} linear relationship. For analysis of the relationship between charge movement and membrane voltage, data points were fitted to a Boltzmann equation of the form $Q = Qmax / [1 + exp(V_{1/2}) Vm) / K]$, where Qmax is the maximal charge; $V_{1/2}$ is the charge half-activation potential; Vm is the membrane potential; and k is the steepness of the curve. For calcium currents, normalized data points to the maximum current amplitude were fitted to the following equation: $I_{Ca} = Gmax(V−Vr)/\{1+ exp[zF(V1/2−V)/RT]\}$, where Gmax is the maximum conductance, V is the membrane potential, Vr is the reversal potential, and $V1/2$ is the half-activation potential, z is the effective valence, F is the Faraday constant, R is the gas constant, and T is the absolute temperature.

Sarcoplasmic reticulum Ca^{2+} release

Dissociated FDB fibers were loaded with Oregon Greeen Bapta-5N (OGB-5N) via the patch pipette as described (Jimenez-Moreno et al., 2008). The dye was allowed to diffuse for 20–30 min before fiber stimulation and after attaining the whole-cell voltage-clamp configuration. Intracellular OGB-5N transients were recorded using a Bio-Rad Radiance 2100 laser scanning

confocal microscope (Zeiss, Oberkochen, Germany). Confocal microscopy allowed us to improve the signal/noise ratio under experimental conditions in which myoplasmic Ca^{2+} concentration was strongly buffered by 20 mM EGTA. This experimental manipulation also ensured a more accurate estimation of the Ca^{2+} release flux. Fibers were imaged through a C-Apochromat 40× water-immersion objective (NA 1.2, Zeiss) or a 20× Fluar (NA 0.75) using an argon laser at 488-nm excitation wavelength. The fluorescence emission was measured at 528 ± 25 nm wavelength. For most experiments, the laser was attenuated to 6–12% with a neutral density filter. Fibers were imaged in line-scan (*x-t*) mode. The fiber was always oriented parallel to the *x* scan direction. Linescan images were acquired with 256 pixels (0.236 μm/pixel) in the *x*- and 512 pixels (0.833 ms/pixel) in the *t*-direction. For image acquisition, we used LaserSharp 2000 software (Bio-Rad, Zeiss), and for the analysis of the image intensity profile, Image J software (NIH, Bethesda, MD). For analysis of the relationship between fluorescence and membrane voltage, data points were fitted to a Boltzmann equation of the form $\Delta F/F = \Delta F/Fmax/[1+exp(V_{1/2}) Vm)/K$, where $\Delta F/F$ max is the maximal normalized fluorescence; $V_{1/2}$ is the $\Delta F/F$ half-activation potential; Vm is the membrane potential; and k is the steepness of the curve.

Statistical analysis

Statistical analysis was performed using the Student's *t* test for paired samples; means were considered statistically significant when the P value was <0.05. The Origin computer program (Microcal Software, Inc., Northampton, MA, USA) was used for statistical analysis.

RESULTS

Figure 1 shows the human and mouse JP-45 amino acid sequences and the location of the *JSRP1* polymorphic variants. We first assessed the frequency of the JP-45 polymorphism in exon 5 and exon 6 in the Swiss MH population, by screening the genomic DNA of patients that had been tested genetically and phenotypically and classified as either MHN (MH negative), MHEh (MH equivocal with abnormal response to halothane) with mutation in *RYR1*, MHEh, with no identified mutation in *RYR1* or MHS (MH susceptible) with a causative *RYR1* mutation. Figure 2 (left panels) shows a schematic representation of the restriction sites generated by the presence of the c.323C>T substitution (top) and of the c.449G>C 6 (bottom). The panels on the right show PCR amplified DNA from individuals with and without the polymorphisms, after digestion with MspA1l (c.323C>T, exon 5) and Acil (c.449G>C exon 6) while the frequency distribution of the polymorphisms among the different individuals is shown in Table 1. As indicated (i) the frequency of the two SNP is not different between individuals belonging to different groups and (ii) the SNP in exon 6 is more frequent compared to that in exon 5. We also identified one MHN individual carrying both polymorphisms.

In order to verify if the *JSRP1* variants influence the resting $[Ca^{2+}]$ and sensitivity of the ryanodine receptor to KCl-induced Ca^{2+} release, we loaded myotubes from MHN/MHE individuals with no *RYR1* mutation, carrying either the p.P108L polymorphism (2 individuals), the p.G150A polymorphism (3 MHN and 3 MHE individuals), with either fura-2 or fluo-4 and studied general aspects of calcium homeostasis. Figure 3A shows that the resting $[Ca^{2+}]_i$ of individuals carrying the p.G150A polymorphism were slightly lower than those carrying either no polymorphism or the p.P108L. It is difficult to interpret if such small changes (<10% of the fura-2 fluorescence value) though statistically significant, could be the consequence of altered

13

EC coupling, in particular due to fine alterations of $Ca_v1.1$ function. We next assessed the response of these myotubes to different concentrations of KCl. As shown in Figure 3B the sensitivity to KCl was very similar in myotubes carrying the p.P108L and p.G150A polymorphism, with an EC_{50} of 36.5±2.5 and 30.5±1.0, respectively but this was shifted to higher KCl concentrations compared to myotubes carrying no polymorphisms (EC_{50} 11.3±6.8), however the peak calcium release induced by KCl or via direct pharmacological activation of the RyR1 with 600 µM 4-chloro-m-cresol, were not different (Figure 3C).

Since JP-45 interacts with $Ca_v1.1$ we investigated in greater detail if the fine functions of the DHPR voltage sensor were affected by the polymorphisms. To this end, we reconstituted FDB muscles from JP-45 KO mice with constructs carrying wild type JP-45 or constructs in which each of the single variants had been inserted, and studied the charge movement, Ca^{2+} currents, and intracellular calcium. Figure 4 (panels A and B) shows the electrophysiological properties of single FDB fibers carrying the different variants. Fibers reconstituted with the cDNA carrying the p.P108L or p.G150A variants showed ~18 mV or more than 20mV displacement of the charge movement-membrane voltage curve toward more positive potentials compared to wild type JP-45 (Table 2). These changes in charge movement were accompanied by significant changes in the voltage-dependence of the calcium current (Fig. 4B). Half activation potential for p.P108L (22 ± 2.8 mV) and p.G150A (23 ± 3.1 mV) was found at more depolarized potentials than wild type JP-45 (2.2 ± 0.41). As the shift in charge movement and calcium current activation for the p.G150A and p.P108L variants was significantly shifted toward more positive potentials compared to wild type JP-45, we examined the voltage-dependence of SR Ca^{2+} release. Consistently, SR Ca^{2+} release shows a ~18 mV shift toward more depolarized potentials induced by both JP-45 variants compared to JP-45 wild type (Fig.

4C and Table 2).

DISCUSSION

In the present paper we investigated the impact of two naturally occurring variants of *JSRP1* on EC coupling and report that their presence downregulates the activity of the dihydropyridine receptor leading to a shift in its sensitivity to activation; thus the presence of polymorphic variants of *JSRP1* and potentially in other genes encoding SR proteins may fine tune skeletal muscle EC coupling and explain the variable phenotypes observed in MHS patients from different genetic backgrounds, with the same *RYR1* mutation.

While analyzing the MHS population, Althobiti et al. (2009) identified two genetic variants of the *JSRP1*, the gene encoding the sarcoplasmic reticulum junctional face membrane protein JP-45, but concluded that it was unlikely that either polymorphism on their own could be causative of malignant hyperthermia and rather such variants may act as modifiers in MH susceptibility. The results of the present study support and extend these findings; analyzing DNA samples collected from 140 individuals of the Swiss population undergoing genetic or functional testing for MH susceptibility, we found that approximately 50% of the population (MHN, MHE and MHS) carried the p.G150A polymorphism, and it is equally distributed among the different MH subgroups. On the other hand the p.P108L polymorphism is much less frequent, being present in only approximately 5% of the total population with no significant difference in its distribution among the different MH subgroups. Nevertheless, the absence of a direct impact of genetic variants on the predisposition to MH as determined by the in vitro contracture test (the gold standard used to determine MH susceptibility) does not exclude an indirect modulatory effect of JP-45 on the fine tuning of EC coupling.

In order to study the functional effects of the JP-45 polymorphisms we used two complementary approaches: (i) we studied calcium homeostasis in myotubes from MHN/MHE individuals negative for *RYR1* mutations and endogenously expressing the variants and (ii) reconstituted skeletal muscles from JP-45 KO mice (Delbono et al., 2007) with either wild type cDNA or the cDNA carrying either variant of JP-45 and studied the electrophysiological characteristics of the DHPR from isolated FDB fibres. Both approaches gave similar results in that the sensitivity of the voltage sensor was shifted to higher depolarizing voltages/KCl concentrations in cells carrying either variant. This result is not totally unexpected as: (i) JP-45 binds directly to the $Ca_v1.1$ through its NH_2-terminal domain and to calsequestrin via its COOH-terminus (Anderson et al., 2006); (ii) over-expression of JP-45 in C_2C_{12} myotubes leads to a reduction of Ca^{2+} permeability per voltage-sensor charge (Gouadon et al., 2006) suggesting that JP-45 down regulates the activity of the EC coupling machinery; (iii) ablation of JP-45 leads to loss of skeletal muscle strength in three months old mice. Interestingly, in an MH mouse animal model ($RYR1_{Y522S}$) Andronache et al. (2009) showed voltage dependence of inactivation of DHPR-mediated Ca^{2+} release were shifted to more negative potentials, indicating that the mice had activated compensatory mechanisms acting on the DHPR to counterbalance the activation of Ca^{2+} release via mutated RyR1 at more negative membrane potentials. We believe that the expression of JP-45 variants represents an additional mechanism counteracting Ca^{2+} release via the RyR1 channel. Indeed in myotubes and reconstituted FDB fibres peak Ca^{2+} release was similar in cells carrying WT or JP-45 variants, but the EC_{50} for depolarization-induced Ca^{2+}–release was shifted by about 20 mM KCl to higher KCl concentrations. Similarly, electrophysiological measurements of fibres reconstituted with JP-45 variants showed that half of the maximal charge movement and Ca^{2+} currents were recorded at more positive potentials

than in fibres reconstituted with wild type JP-45.

Figure 1 shows the human and mouse JP-45 amino acid sequences and the location of the polymorphic variants in a cartoon model. The p.P108L variant falls within a stretch of conserved proline residues which are present in the NH_2 - domain of JP-45; substitution of the helix breaking proline residue for the hydrophobic amino acid leucine may change the structure of the domains interacting with the $Ca_v1.1$ subunit of the DHPR leading to the observed desensitization of the voltage sensor. On the other hand the effect of the more common p.G150A which lies right after the predicted transmembrane domain is more difficult to envisage as both glycine and alanine are neutral nonpolar residues, have a similar isoelectric point (5.95 and 6.0 respectively) but differ in the size of their side-chains (Voet and Voet, 2004). Thus the subsitution of the H^+ side chain on glycine for the CH_3 side group on alanine immediately after the hydrophobic domain may cause conformational changes and/or affect posttranscriptional modifications.

In conclusion we show that the presence of genetic variants of JP-45 affects the function of the voltage sensing dihydropyridine receptor suggesting that variants of other proteins present in the sarcoplasmic reticulum interacting with the RyR1 and /or with the DHPR may similarly affect EC coupling and thus will impact not only the severity of an individual's MH phenotype but potentially also the severity of neuromuscular disorders particularly of the core myopathies.

ACKNOWLEDGMENTS

REFERENCES

Adams BA, Tanabe T, Mikami A, Numa S, Beam KG. 1990. Intramembrane charge movement restored in dysgenic skeletal muscle by injection of dihydropyridine receptor cDNAs. Nature 356: 569-572.

Althobiti M, Booms P, Fiszer D, Halsall PJ, Shaw MA, Hopkins PM. 2009. Sequencing the JSPR1 gene in patients susceptible to malignant hyperthermia and identification of two novel genetic variants. Br J Anaesth 103:321P.

Anderson AA, Treves S, Biral D, Betto R, Sandonà D, Ronjat M, Zorzato F.2003. The novel skeletal muscle sarcoplasmic reticulum JP-45 protein. Molecular cloning, tissue distribution, developmental expression, and interaction with alpha 1.1 subunit of the voltage-gated calcium channel. J Biol Chem 278:39987-39992.

Anderson AA, Altafaj X, Zheng Z, Wang ZM, Delbono O, Ronjat M, Treves S, Zorzato F. 2006.

The junctional SR protein JP-45 affects the functional expression of the voltage-dependent Ca2+ channel Cav1.1. J Cell Sci 119:2145-2155.

Andronache Z, Hamilton SL, Dirksen RT, Melzer W. 2009. A retrograde signal from RyR1 alters DHP receptor inactivation and limits window Ca2+ release in muscle fibers of Y522S RyR1 knock-in mice. Proc Natl Acad Sci USA 106:4531-4536.

Clarke F, Waddell LB, Cooper ST, Perry M, Smith RL, Kornberg AJ, Muntoni, Lillis S, Straub V, Bushby K, Guglieri M, King MD, et al. 2010. Recessive mutations in RYR1 are a common cause of congenital fiber type disproportion. Hum Mutat 31:E1544-1550.

Delbono O. 1992. Calcium current activation and charge movement in denervated mammalian skeletal muscle fibres. J Physiol 451:187-203

Delbono O, Xia J, Treves S, Wang ZM, Jimenez-Moreno R, Payne AM, Messi ML, Briguet A, Schaerer F, Nishi M, Takeshima H, Zorzato F. 2007. Loss of skeletal muscle strength by ablation of the sarcoplasmic reticulum protein JP45. Proc Natl Acad Sci USA 104:20108-20113.

Delbono O, Messi ML, Wang ZM, Treves S, Mosca B, Bergamelli L, Nishi M, Takeshima H, Shi H, Xue B, Zorzato F. 2012. Endogenously determined restriction of food intake overcomes excitation-contraction uncoupling in JP45KO mice with aging. Exp Gerontol 474:304-316.

DiFranco M, Neco P, Capote J, Meera P, Vergara JL. 2006. Quantitative evaluation of mammalian skeletal muscle as a heterologous protein expression system. Protein Expr Purif 47:281-288.

Duarte ST, Oliveira J, Santos R, Pereira P, Barroso C, Conceição I, Evangelista T. 2011. Dominant and recessive RYR1 mutations in adults with core lesions and mild muscle symptoms. Muscle Nerve 44:102-108.

Ducreux S, Zorzato F, Müller C, Sewry C, Muntoni F, Quinlivan R, Restagno G, Girard T, Treves S. 2004. Effect of ryanodine receptor mutations on IL-6 release and intracellular calcium homeostasis in human myotubes from malignant hyperthermia susceptible individuals and patients affected by central core disease. J Biol Chem 279: 43838-43846.

European Malignant Hyperpyrexia Group. 1984. A protocol for the investigation of malignant hyperpyrexia (MH) susceptibility. Br J Anaesth 56:1267-1269.

Fleischer S, Inui M. 1989. Biochemistry and biophysics of excitation–contraction coupling. Annu Rev Biophys Biophys Chem, 18:333–364.

Franzini-Armstrong C, Jorgensen AO. 1994. Structure and development of E–C coupling units in skeletal muscle. Annu Rev Physiol 56:509–534.

Girard T, Urwyler A, Censier K, Müller CR, Zorzato F, Treves S. 2001. Genotype-phenotype comparison of the Swiss malignant hyperthermia population. Hum Mutat 18:357-358.

Glahn KPE, Ellis FR, Halsall PJ, Müller CR, Snoeck MMJ, Urwyler A, Wappler F. 2010. Recognizing and managing a malignant hyperthermia crisis: guidelines from the European Malignant Hyperthermia Group. Br J Anaesth 105:417-420.

Gouadon E, Schuhmeier RP, Ursu D, Anderson AA, Treves S, Zorzato F, Lehmann-Horn F, Melzer W. 2006. A possible role of the junctional face protein JP-45 in modulating Ca2+ release in skeletal muscle. J Physiol 572: 269-280.

Hamill OP, Marty A, Neher E, Sakmann B, Sigworth FJ. 1981. Improved patch-clamp techniques for high resolution current recording from cells and cell-free membrane patches. Pflugers Arch 391:85-100.

Jiménez-Moreno R, Wang ZM, Gerring RC, Delbono O. 2008. Sarcoplasmic reticulum Ca^{2+} release declines in muscle fibers from aging mice. Biophys J 94: 3178-3188.

Jungbluth H, Sewry CA, Muntoni F. 2011. Core myopathies. Semin Pediatr Neurol 18:239-249.

Monnier N, Procaccio V, Stieglitz P, Lunardi J.1997 Malignant-hyperthermia susceptibility is associated with a mutation of the alpha 1-subunit of the human dihydropyridine-sensitive L-type voltage-dependent calcium-channel receptor in skeletal muscle. Am J Hum Genet 60:1316–1325

Nakai J, Dirksen RT, Nguyen HT, Pessah IN, Beam KG, Allen PD. 1996. Enhanced dihydropyridine receptor channel activity in the presence of ryanodine receptor. Nature 380: 72–75.

Pirone A, Schredeklseker J, Tuluc P, Gravino E, Fortunato G, Flucher BE, Carsana A, Salvatore F, Grabner M. 2010. Identification and functional characterization of malignant hyperthermia mutation T1354S in the outer pore of the $Ca_v\alpha_{1S}$-subunit. Am J Physiol 299: C1345-1354.

Rios E, Pizarro G. 1991. Voltage sensor of excitation–contraction coupling in skeletal muscle. Physiol Rev 71:849–908.

Robinson R, Carpenter D, Shaw MA, Halsall J, Hopkins P. 2006. Mutations in RYR1 in malignant hyperthermia and central core disease. Hum Mutat 27:977-989.

Schneider MF, Chandler WK. 1973. Voltage dependent charge movement of skeletal muscle: a possible step in excitation-contraction coupling. Nature 242:244-246.

Stewart SL, Hogan K, Rosenberg H, Fletcher JE. 2001. Identification of the Arg1086His mutation in the alpha subunit of the voltage-dependent calcium channel (CACNA1S) in a North American family with malignant hyperthermia. Clin Genet 59:178-184.

Sutko JL, Airey JA. 1996. Ryanodine receptor Ca2+ release channels: does diversity in form equal diversity in function? Physiol Rev 76: 1027–1071.

Toppin PJ, Chandy TT, Ghanekar A, Kraeva N, Beattie WS, Riazi S. 2010. A report of fulminant malignant hyperthermia in a patient with a novel mutation of the CACNA1S gene. Can J Anesth 57: 689-693.

Treves S, Jungbluth H, Muntoni F, Zorzato F. 2008. Congenital muscle disorders with cores: the ryanodine receptor calcium channel paradigm. Curr Opin Pharmacol 8:319-326.

Treves S, Vukcevic M, Maj M, Thurnheer R, Mosca B, Zorzato F. 2009. Minor sarcoplasmic reticulum membrane components that modulate excitation-contraction coupling in striated muscles. J Physiol 587: 3071-3079.

Treves S, Vukcevic M, Jeannet PY, Levano S, Girard T, Urwyler A, Fischer D, Voit T, Jungbluth H, Lillis S, Muntoni F, Quinlivan R, et al. 2010. Enhanced excitation-coupled Ca^{2+} entry induces nuclear translocation of NFAT and contributes to IL-6 release from myotubes from patients with central core disease. Hum Mol Genet 20589-600.

Voet D and Voet JG. 2004. Biochemistry. 3rd Edition John Wiley and Sons Inc, p 65-79.

Wilmshurst JM, Lillis S, Zhou H, Pillay K, Henderson H, Kress W, Müller CR, Ndondo A, Cloke V, Cullup T, Bertini E, Boennemann C, et al. 2010. RYR1 mutations are a common cause of congenital myopathies with central nuclei. Ann. Neurol 68:717-726.

FIGURE LEGENDS

Figure 1: Comparison of the amino acid sequences of human and mouse JP-45 and location of the polymorphic variants.

Figure 2: *Left* - schematic representation of DNA fragments from wild type and polymorphic variants of JP-45 showing size of fragments and location of restriction sites. *Right*- representative polyacrylamide gel from a wild type (-) and carrier of JP-45 variants after PCR amplification and restriction enzyme digestion. PCR conditions and primers were as described in the Materials and Methods section.

Figure 3: **Calcium regulation in myotubes from individuals carrying wild type or polymorphic variants of JP-45**. **A**- resting fura-2 fluorescent ratio. The resting $[Ca^{2+}]_i$ concentration was slightly but significantly reduced in cells from individuals carrying the p.G150A polymorphism. **B**- KCl induced Ca^{2+} release curves in myotubes from control individuals (pooled from 3 MHN individuals; *_____*), from individuals carrying the p.P108L JP-45 variant (pooled from 2 MHN individuals O - - - O); and from individuals carrying the p.G150A JP-45 variant (pooled values from 3 MHN and 3 MHEh with no *RYR1* mutation □-.-.-.-.□). Each point represents the mean (±S.E.M.) percent increase in fluo-4 fluorescence obtained at the indicated KCl concentration calculated with respect to the value obtained by stimulating

24

myotubes with 100 mM KCl (n=5-12 averaged values per point). **C-** peak increase in fura-2 fluorescence ratio induced by 60 mM KCl (light grey boxes) and 600 μM 4-chloro-m-cresol (dark boxes); results are the mean (± SEM) of 9-12 measurements.

Figure 4: Charge movement, calcium current, and SR Ca^{2+} release in wild type JP-45 and JP-45 variants. **A**. Normalized charge movement to maximal charge (Qmax)-Vm relationship. Data points were fitted to a Boltzmann equation (Methods) and best fitting parameters are included in Table 2 (n = 8-14 fibers from 4-5 mice per group). **B**. Normalized Calcium current (I$_{ca}$)-Vm. Data points were normalized to peak current as described (Methods) (n = 7-13 fibers per group from 4 mice per group). **C**. Normalized Oregon Green Bapta (OGB)-5N-Vm relationship (n = 8-11 fibers from 3-4 mice per group).
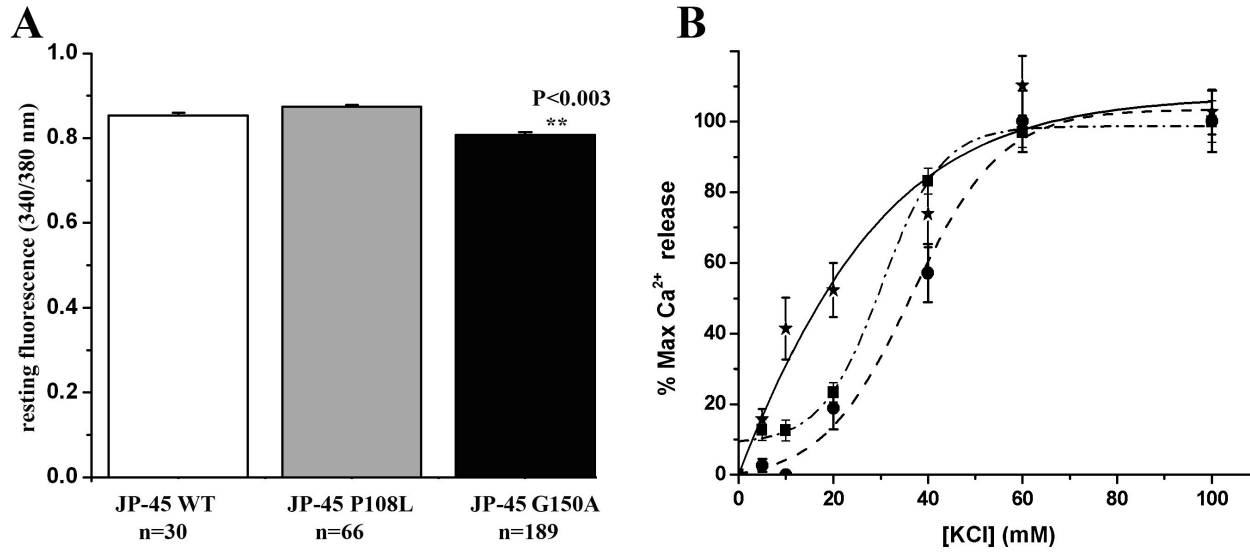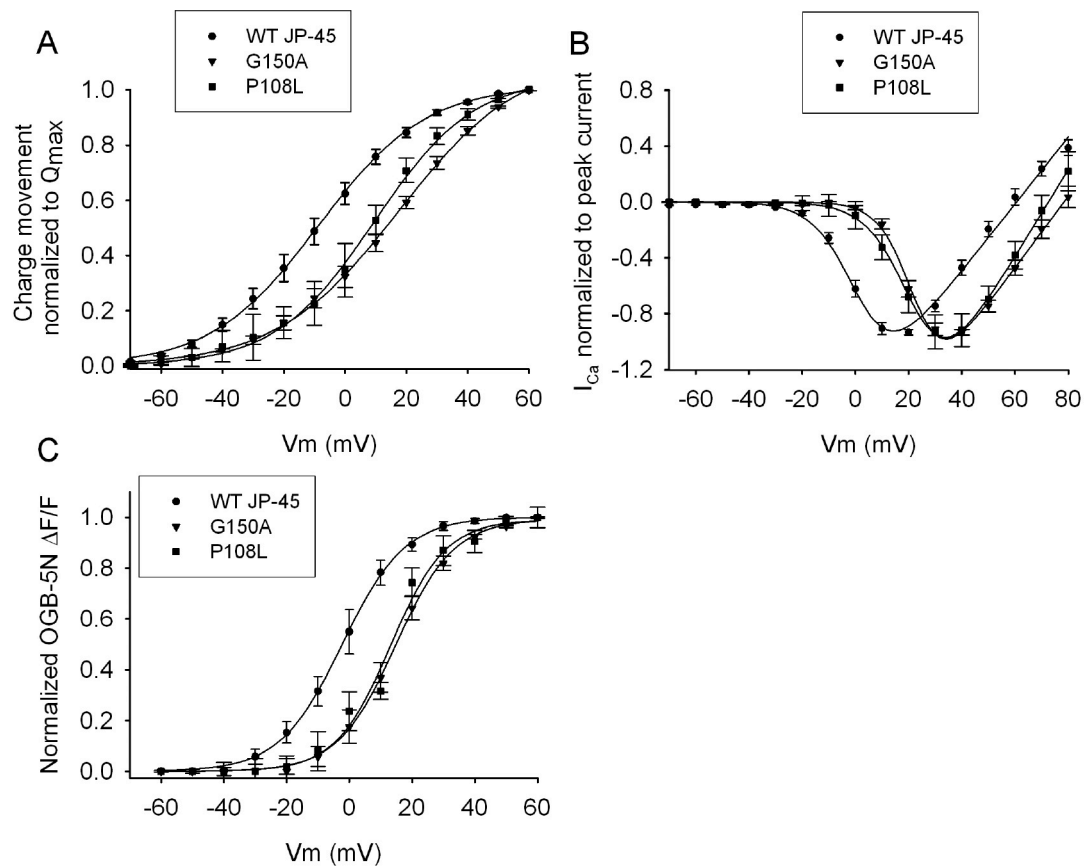
Figure 1
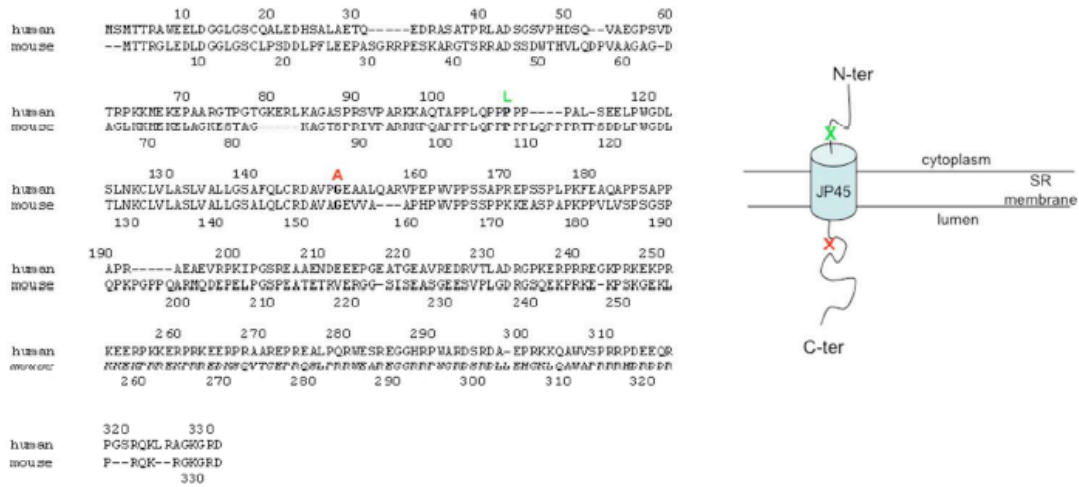
Figure 2
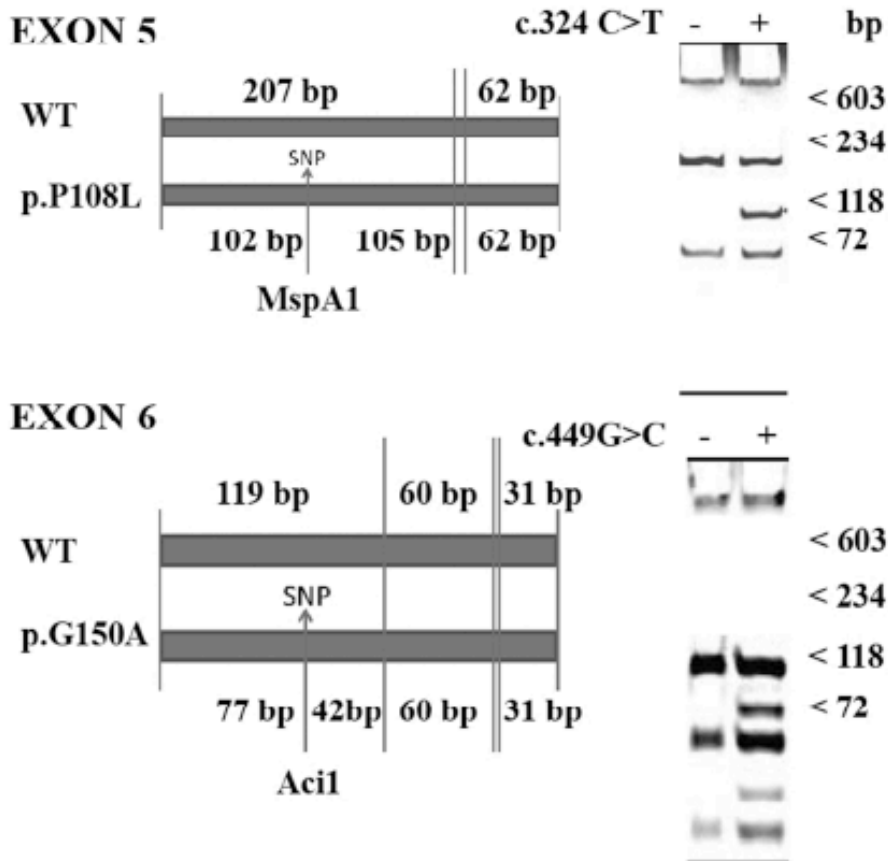
Figure 3

Figure 4

Table 1:

Table 1: Frequency of JP-45 polymorphisms in the Swiss MH population

	MHN	MHEh Mutation (-)	MHEh Mutation (+)	MHS
Exon 5 (p.P108L)	2/63 (3%)	1/13 (8%)	0/7 (0%)	2/57 (3 %)
Exon 6 (p.G150A)	24/63 (38%)	7/13 (54%)	3/7 (43%)	20/57 (35%)

The frequency of the two SNP is not different between MHN and MHS groups.

Table 2:

Table 2

Best fitting parameters describing the voltage-dependence of charge movement and changes in the $[Ca^{2+}]_i$ in FDB fibers

	Charge Movement		
	Maximal Q (nC/µF)	$V_{1/2}$ (mV)	K
WT JP-45	26 ± 2.9	-8.6 ± 1.1	18 ± 1.2
p.P108L	24 ± 2.6	9.7±0.9 *	16 ±1.3
p.G150A	26 ± 3.1	18 ± 2.1 *	20 ± 1.6
	Intracellular Calcium		
	Maximal ΔF/F	$F_{V1/2}$ (mV)	K
WT JP-45	0.61 ± 0.07	-2.3 ± 0.33	10 ± 2.1
p.P108L	0.58 ± 0.03	14 ± 3.1*	8.8 ± 2.6
p.G150A	0.55 ± 0.06	16 ± 2.8 *	9.3 ± 1.9

Q: charge movement, F: fluorescence; $V_{1/2}$: half-activation potential; K: curve steepness. * $P <$ 0.01 for p.G150A or p.P108L *vs* wild type (WT). Charge movement, n = 8-14 fibers from 4-5 mice per group; calcium current, n = 7-13 fibers per group from 4 mice per group; and intracellular calcium, n = 8-11 fibers from 3-4 mice per group).